A longitudinal study on resting state functional connectivity in behavioral variant frontotemporal dementia and Alzheimer's disease

Anne Hafkemeijer[a,b,c*], Christiane Möller[d], Elise G. P. Dopper[b,d,e], Lize C. Jiskoot[b,e,f], Annette A. van den Berg-Huysmans[b], John C. van Swieten[e,g], Wiesje M. van der Flier[d,h], Hugo Vrenken[i,j], Yolande A. L. Pijnenburg[d], Frederik Barkhof[i], Philip Scheltens[d], Jeroen van der Grond[b], and Serge A. R. B. Rombouts[a,b,c]

[a] Department of Methodology and Statistics, Institute of Psychology, Leiden University, 2300 RB Leiden, The Netherlands
[b] Department of Radiology, Leiden University Medical Center, Postzone C2-S, PO Box 9600, 2300 RC Leiden, The Netherlands
[c] Leiden Institute for Brain and Cognition, Leiden University, 2300 RC Leiden, The Netherlands
[d] Alzheimer Center & Department of Neurology, VU University Medical Center, PO Box 7057, 1007 MB Amsterdam, The Netherlands
[e] Alzheimer Center & Department of Neurology, Erasmus Medical Center, PO Box 2040, 3000 CA Rotterdam, The Netherlands
[f] Department of Neuropsychology, Erasmus Medical Center, PO Box 2040, 3000 CA Rotterdam, The Netherlands
[g] Department of Clinical Genetics, VU University Medical Center, PO Box 7057, 1007 MB Amsterdam, The Netherlands
[h] Department of Epidemiology and Biostatistics, VU University Medical Center, PO Box 7057, 1007 MB Amsterdam, The Netherlands
[i] Department of Radiology and Nuclear Medicine, VU University Medical Center, PO Box 7057, 1007 MB Amsterdam, The Netherlands
[j] Department of Physics and Medical Technology, VU University Medical Center, PO Box 7057, 1007 MB Amsterdam, The Netherlands

Running title: Longitudinal connectivity in bvFTD and AD

Keywords: AD; Alzheimer's disease; Frontotemporal dementia; Frontotemporal lobar degeneration; FTD; Functional connectivity; Longitudinal; Resting state fMRI; Resting state networks

*** Correspondence to:** Anne Hafkemeijer, Department of Radiology, Leiden University Medical Center, Postzone C2-S, PO Box 9600, 2300 RC Leiden, The Netherlands Tel.: +31 71 526 3998
Email: A.Hafkemeijer@lumc.nl

Email addresses:
A.Hafkemeijer@lumc.nl; C.Moeller@vumc.nl; E.Dopper@erasmusmc.nl; L.C.Jiskoot@erasmusmc.nl; A.A.van_den_Berg-Huysmans@lumc.nl; J.C.vanSwieten@erasmusmc.nl; WM.vdFlier@vumc.nl; H.Vrenken@vumc.nl; Y.Pijnenburg@vumc.nl; F.Barkhof@vumc.nl; P.Scheltens@vumc.nl; J.van_der_Grond@lumc.nl; S.A.R.B.Rombouts@lumc.nl

Checklist

Title:	131 characters
Running title:	41 characters
Keywords:	9 words
Total:	5567 words
Summary:	270 words
References:	64
Table:	Table 1, Table 2, Supplementary Table 1
Figures:	Figure 1, Figure 2, Figure 3, Figure 4, Figure 5, Figure 6, and Supplementary Figure 1 (all color)

Abbreviations

AD:	Alzheimer's disease
bvFTD:	behavioral variant of Frontotemporal Dementia
CDR:	Clinical Dementia Rating Scale
FAB:	FMRIB's ICA-based Xnoiseifier
fMRI:	Functional Magnetic Resonance Imaging
FSL:	Functional Magnetic Resonance Imaging of the Brain Software Library
FWE:	Family-Wise Error
GDS:	Geriatric Depression Scale
GLM:	General Linear Model
ICA:	Independent Component Analysis
MMSE:	Mini-Mental State Examination
MNI:	Montreal Neurological Institute
MRI:	Magnetic Resonance Imaging
TFCE:	Threshold-Free Cluster Enhancement
VBM:	Voxel-Based Morphometry

Abstract

Background and objective: Alzheimer's disease (AD) and behavioral variant frontotemporal dementia (bvFTD) are the most common types of early-onset dementia. We applied longitudinal resting state fMRI to delineate functional brain connections relevant for disease progression and diagnostic accuracy.

Methods: We used two-center resting state fMRI data of 20 AD patients (65.1±8.0 years), 12 bvFTD patients (64.7±5.4 years), and 22 control subjects (63.8±5.0 years) at baseline and 1.8-year follow-up. We used whole-network and voxel-based network-to-region analyses to study group differences in functional connectivity at baseline and follow-up, and longitudinal *changes* in connectivity within and between groups.

Results: At baseline, connectivity between paracingulate gyrus and executive control network, between cuneal cortex and medial visual network, and between paracingulate gyrus and salience network was higher in AD compared with controls. These differences were also present after 1.8 years. At follow-up, connectivity between angular gyrus and right frontoparietal network, and between paracingulate gyrus and default mode network was lower in bvFTD compared with controls, and lower compared with AD between anterior cingulate gyrus and executive control network, and between lateral occipital cortex and medial visual network. Over time, connectivity decreased in AD between precuneus and right frontoparietal network and in bvFTD between inferior frontal gyrus and left frontoparietal network. Longitudinal changes in connectivity between supramarginal gyrus and right frontoparietal network differ between both patient groups and controls.

Conclusion: We found disease-specific brain regions with longitudinal connectivity changes. This suggests the potential of longitudinal resting state fMRI to delineate regions relevant for disease progression and for diagnostic accuracy, although no group differences in longitudinal changes in the direct comparison of AD and bvFTD were found.

Introduction

Alzheimer's disease (AD) and behavioral variant frontotemporal dementia (bvFTD) are the most common types of early-onset dementia [1]. AD is mainly characterized by deficits in episodic and working memory [2], whereas patients with bvFTD typically present with changes in behavior [3].

A substantial amount of dementia research used neuroimaging to elucidate the pathophysiology of bvFTD and AD [4,5]. Imaging of brain structure shows typical AD atrophy in the hippocampus, precuneus, posterior cingulate cortex, parietal, and occipital brain regions [6–8]. In bvFTD, atrophy is most often found in the anterior cingulate cortex, frontoinsula, and frontal brain regions [7,8].

Longitudinal studies have shown to be useful to elucidate changes in gray matter volume over time, showing that in AD atrophy progresses faster in the hippocampus and posterior cingulate cortex, while atrophy progresses faster in the orbitofrontal gyrus and frontal lobe in bvFTD [7,9–11]. These studies show the importance of longitudinal designs to delineate regions relevant for disease progression.

The disease-specific patterns of gray matter atrophy show spatial overlap with functional brain networks [8]. Imaging of these functional networks offers the opportunity to study brain function and dysfunction in AD and bvFTD [8,12]. AD patients show abnormalities in functional network connectivity in the posterior hippocampal-cingulo-temporal-parietal network known as the default mode network [13–16]. Patients with bvFTD show functional connectivity abnormalities in the anterior frontoinsular-cingulo-orbitofrontal network often called the salience network [16–21].

Despite evidence from cross-sectional studies that functional network connectivity gives the opportunity to study brain dysfunction in dementia and therefore has potential to study disease progression, little is known about how functional connections change over time in AD and bvFTD. Studying longitudinal functional connectivity is important to monitor disease progression and may

have utility to improve differential diagnosis of both types of dementia. The aim of the present study was to delineate functional connections relevant for disease progression and diagnostic accuracy. We used longitudinal resting state functional magnetic imaging (fMRI) data of AD and bvFTD patients to investigate, in addition to cross-sectional group differences, longitudinal changes in functional connectivity within and between groups.

Materials and methods

Participants

We included 20 patients with probable AD, 12 patients with probable bvFTD, and 22 control participants (Table 1). All subjects were recruited from two Dutch centers specialized in dementia: the Alzheimer Center of the VU University Medical Center Amsterdam, and the Alzheimer Center of the Erasmus University Medical Center Rotterdam.

All patients underwent a standardized dementia screening including medical history, informant-based history, physical and neurological examination, blood tests, extensive neuropsychological assessment, and magnetic resonance imaging (MRI) of the brain. In total 5 patients were treated with anticholinesterase medication and 5 patients with psychotropic medication (anxiolytics or antidepressants). Diagnoses were established in a multidisciplinary consensus meeting according to the core clinical criteria of the National Institute on Aging and the Alzheimer's Association workgroup for probable AD [2,22] and according to the clinical diagnostic criteria for bvFTD [3]. To minimize center effects, all diagnoses were re-evaluated in a panel including clinicians from both Alzheimer centers.

The control participants were screened to exclude memory complaints, drug or alcohol abuse, major psychiatric disorders, and neurological or cerebrovascular diseases. They underwent an assessment including medical history, physical examination, extensive neuropsychological assessment, and an MRI of the brain, comparable to the work-up of patients.

All study participants underwent extensive neuropsychological assessment and MRI scanning at baseline and follow-up (Supplementary Table 1). Mean interval between the first visit (baseline measurement) and second visit (follow-up measurement) was 1.8 years (1.79 years for AD patients, 1.76 years for bvFTD patients, and 1.77 years for controls).

This study was performed in compliance with the Code of Ethics of the World Medical Association (Declaration of Helsinki). Ethical approval was obtained from the local ethics committees. Written informed consent from all participants was obtained.

Data acquisition

All participants underwent an MRI of the brain, on a 3 Tesla scanner using a standard 8-channel head coil, either in the VU University Medical Center (Signa HDxt, GE Healthcare, Milwaukee, WI, USA), or in the Leiden University Medical Center (Achieva, Philips Medical Systems, Best, The Netherlands) at baseline and follow-up.

Resting state fMRI T2*-weighted scans were acquired using whole brain multislice gradient echo planar imaging. Imaging parameters in the VU University Medical Center were: TR = 1.8 sec, TE = 35 msec, flip angle = 80°, 34 slices, resulting in a voxel size of 3.30 x 3.30 x 3.30 mm, including 10% interslice gap, 200 volumes, scan duration 6 minutes. Imaging parameters in the Leiden University Medical Center were: TR = 2.2 sec, TE = 30 msec, flip angle = 80°, 38 slices, resulting in a voxel size of 2.75 x 2.75 x 2.99 mm, including 10% interslice gap, 200 volumes, scan duration 7 minutes and 33 seconds. Participants were instructed to lie still with their eyes closed and not to fall asleep during the resting state scan.

Three-dimensional T1-weighted anatomical images were acquired, for registration purposes and to study group differences in gray matter volume. Imaging parameters in the VU University Medical Center were: TR = 7.8 msec, TE = 3 msec, flip angle = 12º, 180 slices, resulting in a voxel size of 0.98 x 0.98 x 1.00 mm. Imaging parameters in the Leiden University Medical Center were: TR = 9.8 msec, TE = 4.6 msec, flip angle = 8°, 140 slices, resulting in a voxel size of 0.88 x 0.88 x 1.20 mm. In the Leiden University Medical Center an additional high-resolution echo planar imaging scan was acquired for registration purposes (TR = 2.2 sec, TE = 30 msec, flip angle = 80°, 84 slices, resulting in a voxel size of 1.96 x 1.96 x 2.00 mm, including 10% interslice gap).

In addition, the MRI protocol included a 3D Fluid Attenuated Inversion Recovery (FLAIR) sequence, dual-echo T2-weighted sequence, and susceptibility weighted imaging (SWI) which were reviewed for brain pathology other than atrophy by an experienced radiologist. White matter hyperintensities were rated using the Fazekas scale [23]. Subjects with a score higher than 2 were excluded.

Data analysis

Before analysis, all MRI scans were submitted to a visual quality control check to ensure that no gross artifacts were present in the data. Data analysis was performed with Functional Magnetic Resonance Imaging of the Brain Software Library (FSL 5.0.1, Oxford, United Kingdom) [24]. Anatomical regions were determined using the Harvard-Oxford cortical and subcortical structures atlas integrated in FSL.

Gray matter volume

Structural MRI scans were analyzed with voxel-based morphometry (VBM) analysis [25] to study group differences and longitudinal changes in gray matter volume. First, the structural images were brain extracted and tissue-type segmented [26]. The resulting gray matter partial volume images were aligned to the gray matter MNI-152 standard space image (Montreal Neurological Institute, Montreal, QC, Canada) [27], followed by non-linear registration [28]. The images were averaged to create a study-specific template. Next, all native gray matter images were non-linearly registered to this study-specific gray matter template [25,29]. To correct for the contractions and enlargements due to the non-linear registration, each voxel of each registered gray matter image was multiplied by the Jacobian of the warp field, which defines the direction and the amount of modulation. The modulated segmented images were spatially smoothed with an isotropic Gaussian kernel with a full width at half maximum of 7 mm.

We studied 1) cross-sectional group differences at baseline (Fig. 1.1), 2) cross-sectional group differences at follow-up (Fig. 1.2), 3) longitudinal *changes* in gray matter volume within groups (i.e., is, within each group, the gray matter volume at follow-up different from that at baseline (delta)?)

(Fig. 1.3), 4) group differences in longitudinal *changes* in gray matter volume (i.e., are the deltas different between groups?) (Fig. 1.4). To study group differences in gray matter volume at baseline and at follow-up, a general linear model (GLM) approach using analysis of variance F-tests with post hoc Bonferroni adjusted t-tests was applied. Age, gender, study center, and duration of symptoms were included as covariate in the statistical model. To study longitudinal *changes* in gray matter volume, individual gray matter maps from the second visit (follow-up) were subtracted from the corresponding gray matter maps from the first visit (baseline). This results for each subject in a map containing the differences in gray matter volume between the two time points (delta). These maps were concatenated across subjects into single 4D maps and were submitted to voxel-based statistical testing to study longitudinal changes in gray matter volume within (Fig. 1.3) and between groups (Fig. 1.4). F-tests were used adjusted for age, gender, study center, and duration of symptoms with post hoc t-tests. Voxel-wise non-parametric permutation testing [30] with 5000 permutations was performed using FSL-randomise correcting for multiple comparisons across voxels (statistical threshold set at $p < 0.05$, Family-Wise Error (FWE) corrected), using the Threshold-Free Cluster Enhancement (TFCE) technique [31].

Preprocessing of resting state fMRI data

The preprocessing of the resting state data consisted of motion correction [27], brain extraction [32], spatial smoothing using a Gaussian kernel with a full width at half maximum of 3 mm, and high-pass temporal filtering (cutoff frequency of 0.01 Hz). After preprocessing, the functional images were registered to the corresponding T1-weighted images using Boundary-Based Registration [33]. T1-weighted images were registered to the 2 mm isotropic MNI-152 standard space image (Montreal Neurological Institute, Montreal, QC, Canada) using nonlinear registration [34] with a warp resolution of 10 mm. High-resolution echo planar images (only available for subjects scanned in the Leiden University Medical Center) were used for an additional registration step between functional images and T1-weighted images. In order to achieve better comparison across voxels, subjects, time points, and centers, standardization on a voxel-by-voxel basis has been recommended [35]. We used the Z-standardization approach in which individual resting state fMRI time series were normalised

(standardized to z-scores) on a voxel-by-voxel basis using the mean and standard deviation of each individual resting state signal across time (previously described in [35]). Single-session independent component analysis (ICA) was performed on the preprocessed resting state data to decompose the data into distinct components for denoising purposes [36]. FMRIB's ICA-based Xnoiseifier 1.05 (FIX) was used to auto-classify ICA components into "good" (i.e., functional signal) and "bad" (i.e., noise) components [37]. FIX removed unique variance related to "noise" components and motion confounds from the preprocessed fMRI data to denoise the resting state data and to increase the signal-to-noise ratio.

Resting state networks of interest

Group differences and longitudinal changes in functional connectivity were studied using the dual regression method of FSL (previously described in [38]). We used standard resting state networks as a reference to study functional connectivity in a standardized way [39,40]. Resting state functional connectivity was determined in terms of similarity of the BOLD fluctuations in the brain in relation to characteristic fluctuations in the predefined resting state networks [41,42]. These standardized resting state networks parcellate the brain into nine templates: network I) calcarine sulcus, precuneal cortex, and primary visual cortex (medial visual network); network II) superior and fusiform areas of lateral occipital cortex (lateral visual network); network III) superior temporal cortex, insular cortex, anterior cingulate cortex, auditory cortex, operculum, somatosensory cortices, thalamus (auditory system network); network IV) precentral and postcentral somatosensory somatomotor areas (sensorimotor system network); network V) rostal medial prefrontal cortex, precuneal cortex, posterior cingulate cortex (default mode network); network VI) medial and inferior prefrontal cortex, anterior cingulate and paracingulate gyri, prefrontal cortex (executive control network); networks VII and VIII) frontal pole, dorsolateral prefrontal cortex, parietal lobule, paracingulate gyrus, posterior cingulate cortex (right and left frontoparietal network), additionally we studied connectivity with network IX) anterior cingulate cortex, insular cortex, frontal orbital cortex, and frontal pole (salience network) (for further details see Fig. 3A and [42–44]). To account for noise, even after FIX, white matter and cerebrospinal fluid templates were included in the analysis [45–47].

In the dual regression, individual time series were first extracted for each template, using the resting state networks [42,44] and the two additional white matter and cerebrospinal fluid maps [45–47], in a spatial regression against the individual fMRI data set (regression 1). The resulting matrices described temporal dynamics for each template and individual. Next, the temporal regressors were used to fit a linear model to the individual fMRI data set (regression 2), to estimate the spatial maps for each individual. This results in 3D images for each individual, with voxel-wise z-scores representing the functional connectivity to each of the templates. The higher the absolute value of the z-score, the stronger the connectivity to a network. Here, we studied 1) mean network connectivity (z-score) within the resting state networks of interest, and 2) network-to-region connectivity using a more detailed voxel-based analysis.

Mean network connectivity

First, we performed a whole-network analysis to study mean functional connectivity within each network of interest. For each participant, mean functional connectivity (z-score) per network was calculated. Figure 1 shows the statistical analyses that were performed. We studied 1) cross-sectional group differences at baseline (Fig. 1.1), 2) cross-sectional group differences at follow-up (Fig. 1.2), 3) longitudinal *changes* in connectivity within groups (i.e., is, within each group, the functional connectivity at follow-up different from that at baseline (delta)?) (Fig. 1.3), 4) group differences in longitudinal *changes* in connectivity (i.e., are the deltas different between groups?) (Fig. 1.4). We used analysis of covariance (ANCOVA; general linear model (GLM) procedure), adjusted for age, gender, study center, and duration of symptoms with post hoc Bonferroni adjusted t-tests (IBM SPSS Statistics Version 20, IBM Corp. Somers, NY, USA), to study cross-sectional group differences in mean network connectivity at baseline and at follow-up. We performed these analyses both without and with a correction for total gray matter volume of each network (at baseline or follow-up). To study longitudinal *changes* in mean network connectivity, individual mean z-score per network from the second visit (follow-up) were subtracted from the corresponding mean z-score from the first visit (baseline). This results in a delta score between the two time points per network for each subject. These delta scores were tested using an ANCOVA, adjusted for age, gender, study center, duration of

symptoms, and network connectivity at baseline, with post hoc Bonferroni adjusted t-tests, to study longitudinal changes in network connectivity within and between groups. These analyses were performed both without and with a correction for longitudinal changes in total gray matter volume of each network. Statistical threshold was set at $p < 0.05$ for all statistical tests.

Network-to-region connectivity

In a second, more detailed voxel-based analysis, we studied functional connectivity between resting state networks and localized brain regions. We used a GLM approach, as implemented in FSL, using F-tests, adjusted for age, gender, study center, and duration of symptoms with post hoc t-tests, to study cross-sectional group differences at baseline (Fig. 1.1) and at follow-up (Fig. 1.2). We performed these analyses both without and with a correction for voxel-based gray matter volume (at baseline or follow-up). To study longitudinal *changes* in network-to-region connectivity, individual functional connectivity maps (parameter estimates) from the second visit (follow-up) were subtracted from the corresponding functional connectivity maps from the first visit (baseline). This results for each subject in a map containing, per network, the differences in functional connectivity between the two time points (delta). These maps were concatenated across subjects into single 4D maps (one per predefined network) and were submitted to voxel-based statistical testing to study longitudinal changes in network-to-region connectivity within (Fig. 1.3) and between groups (Fig. 1.4). F-tests were used adjusted for age, gender, study center, and duration of symptoms with post hoc t-tests. These analyses were performed both without and with a correction for longitudinal voxel-based gray matter changes (i.e., delta gray matter volume). Per network, the statistical analyses were masked by the baseline one-sample map from the control group for that network. Voxel-wise non-parametric permutation testing [30] with 5000 permutations was performed using FSL-randomise correcting for multiple comparisons across voxels (statistical threshold set at $p < 0.05$, Family-Wise Error (FWE) corrected), using the Threshold-Free Cluster Enhancement (TFCE) technique [31].

Associations with cognitive performance

In a final analysis, we investigated the possible associations between changes in network-to-region connectivity and longitudinal changes in cognitive performance (i.e., Mini Mental State Examination (MMSE) score [48] and Frontal Assessment Battery (FAB) scores [49]), using linear regression analyses (IBM SPSS Statistics Version 20, IBM Corp. Somers, NY, USA), adjusted for age, gender, study center, and duration of symptoms (statistical threshold was set at $p < 0.05$).

Results

Demographic characteristics

Demographic data for all participants are summarized in Table 1. There were no differences between patient groups with regard to age at baseline, follow-up time, gender, study center distribution, level of education, and duration of symptoms. As expected, both dementia groups performed worse on cognitive tests compared with controls (all $p < 0.05$). Patients with AD performed worse at follow-up compared with baseline on MMSE ($p = 0.016$) and FAB ($p = 0.049$). Results of extensive neuropsychological assessment are shown in Supplementary Table 1.

Gray matter volume

Voxel-wise structural analysis at baseline revealed group differences in gray matter volume (Fig. 2A-B). Patients with AD showed less gray matter in posterior cingulate cortex, precuneal cortex, frontal medial cortex, temporal gyrus, hippocampus, and frontal orbital cortex compared with controls (Fig. 2A). Patients with bvFTD showed less gray matter in anterior cingulate cortex, insular cortex, and temporal pole compared with controls (Fig. 2B). No baseline differences in gray matter volume were found between patients with AD and patients with bvFTD. These differences in gray matter volume were also found at follow-up (Fig. 2C-D). Longitudinal gray matter analyses showed over time decreased gray matter in the precuneal cortex, posterior cingulate cortex, temporal gyrus, parahippocampal gyrus, and accumbens in the AD group (Fig. 2E) and in the insular cortex, anterior cingulate cortex, and temporal gyrus in the bvFTD group (Fig. 2F).

Mean network connectivity

We performed a whole-network analysis to study mean network functional connectivity in the nine resting state networks of interest (Fig. 3A). These analyses were performed both without and with correction for total gray matter volume of each network.

At baseline (Fig. 1.1), we found significant group differences in network VII and VIII. The results of post hoc testing showed lower mean connectivity in the right and left frontoparietal network (which include parietal lobule, paracingulate and postcingulate gyrus, and frontal pole) in the AD group compared with the control group ($p = 0.045$, $p = 0.008$, both uncorrected for gray matter volume) (Fig. 3B). When a correction for gray matter volume was applied functional connectivity in network VII (right frontoparietal network) was lower in the AD group compared with the control group ($p = 0.024$, gray matter corrected). No baseline differences in mean network connectivity were found in the bvFTD group.

At follow-up (Fig. 1.2), significant group differences were found in mean network connectivity in network VII. Post hoc testing showed lower connectivity in this right frontoparietal network in AD compared with controls ($p = 0.010$, uncorrected for gray matter volume) and in bvFTD compared with controls ($p = 0.012$, uncorrected for gray matter volume) (Fig. 3B). When a correction for gray matter volume was applied functional connectivity in network VII (right frontoparietal network) was lower in the AD group compared with the control group ($p = 0.005$, gray matter corrected) and in bvFTD compared with controls ($p = 0.009$, gray matter corrected).

When longitudinal *changes* in mean network connectivity were studied (Fig. 1.3), we found decreased mean connectivity in network VIII (left frontoparietal network) after the 1.8-year follow-up period in the bvFTD group ($p = 0.021$, uncorrected for gray matter volume) (Fig. 3B). No longitudinal changes in the bvFTD group were found when a gray matter volume correction was applied. In the AD and control group, no longitudinal changes in mean network connectivity were found.

When group differences in longitudinal *changes* were studied (Fig. 1.4), we found with post hoc tests group differences in longitudinal changes in mean network connectivity in network VII (right frontoparietal network) between AD and controls ($p = 0.041$, uncorrected for gray matter volume), and between bvFTD and controls ($p = 0.043$, uncorrected for gray matter volume). When a correction for gray matter volume was applied, longitudinal changes in mean network connectivity were found

in network VII (right frontoparietal network) between AD and controls (p = 0.031, gray matter corrected), and between bvFTD and controls (p = 0.043, gray matter corrected). The mean connectivity in this network decreased more in AD and bvFTD patients than in controls.

Network-to-region connectivity

In a more detailed voxel-based analysis, we studied functional connectivity between the nine resting state networks of interest (Fig. 3A) and localized brain regions (Fig. 4).

At baseline (Fig. 1.1), we found significant group differences in network-to-region connectivity within four resting state networks: networks I, III, VI, and IX (Fig 4A, indicated in light orange). The results of post hoc testing showed higher functional connectivity in AD compared with controls between the lingual gyrus and network I (medial visual network), between the central opercular gyrus and network III (auditory system network), between the paracingulate gyrus and network VI (executive control network), and between the paracingulate gyrus and network IX (salience network) (Fig. 4A, AD > HC, yellow-to-red voxels, Table 2). No baseline differences in network-to-region connectivity were found in the bvFTD group. When a voxel-based correction for gray matter volume was applied comparable group differences in functional connectivity were found (Supplementary Figure 1, and Table 2 right column).

At follow-up (Fig. 1.2), significant group differences in network-to-region connectivity were found in six resting state networks: networks I, III, V, VI, VII, IX (Fig. 4B, indicated in light orange). Post hoc testing showed that the baseline differences in functional connectivity between AD patients and controls were also present at the 1.8-year follow-up measurement (Fig. 4B, AD > HC, yellow-to-red voxels). Note the lateralization of the effect in network III at follow-up. This lateralization was not visible in the images that were not corrected for FWE (uncorrected images not shown). The results of post hoc testing showed also group differences that were only present at follow-up: functional connectivity was lower in AD compared with controls between the angular gyrus and network VII (right frontoparietal network) (Fig. 4B, AD < HC, light-to-dark blue voxels), and in bvFTD between

the paracingulate gyrus and network V (default mode network), and between the angular gyrus and network VII (right frontoparietal network) (Fig. 4B, FTD < HC, light-to-dark blue voxels, Table 2). Functional connectivity in bvFTD was lower compared with AD patients between the lateral occipital cortex and network I (medial visual network), and between the anterior cingulate gyrus and network VI (executive control network) (Fig. 4B, FTD < AD, light-to-dark blue voxels, Table 2). After voxel-based correction for gray matter volume comparable group differences in functional connectivity were found (Supplementary Figure 1, and Table 2 right column).

When longitudinal *changes* in network-to-region connectivity were studied (Fig. 1.3), we found decreased connectivity over time within two networks: network VII and VIII (Fig. 5, indicated in light orange). In the AD group, functional connectivity between the precuneus and network VII (right frontoparietal network) decreased over time (Fig. 5A, and D). In the bvFTD group, functional connectivity between the supramarginal gyrus and network VII (right frontoparietal network), and between the inferior frontal gyrus and network VIII (left frontoparietal network) decreased over time (Fig. 5B-D). No longitudinal changes in network-to-region connectivity were found in the control group. After voxel-based correction for longitudinal gray matter changes comparable functional connectivity changes were found.

When group differences in longitudinal *changes* were studied (Fig. 1.4), we found group differences in longitudinal changes in network-to-region connectivity in network VII (Fig. 6, indicated in light orange). The results of post hoc testing showed group differences in longitudinal changes in connectivity between the supramarginal gyrus and network VII (right frontoparietal network) in AD (Fig. 6A, AD versus HC), and in bvFTD (Fig. 6B, FTD versus HC) when compared with controls. These small brain clusters show a decrease in functional connectivity over time in both patients groups, and an (insignificant) increase in the control group (Fig. 6C). Comparable functional connectivity changes were found when a voxel-based correction for longitudinal gray matter changes was applied.

Associations with cognitive performance

Finally, we studied whether the changes in network-to-region connectivity within groups (i.e. decreased connectivity with the precuneus in AD (Fig. 5A), and with the supramarginal (Fig. 5B) and inferior frontal gyrus (Fig. 5C) in bvFTD) were associated with changes in cognitive performance. In AD, no associations between changes in MMSE scores and changes in precuneal connectivity were found ($p = 0.894$). Changes in FAB scores were not associated with changes in supramarginal ($p = 0.310$) and inferior frontal gyrus ($p = 0.694$) connectivity in bvFTD.

Discussion

In this longitudinal study on resting state fMRI data in AD and bvFTD, we used whole-network and network-to-region analyses to study group differences in functional connectivity at baseline and at 1.8-year follow-up measurement, and *changes* in functional connectivity over time. We found disease-specific brain regions with longitudinal changes in functional connectivity in AD and bvFTD. Over time, the connectivity between precuneus and right frontoparietal network decreased in AD, whereas in bvFTD connectivity between inferior frontal gyrus and left frontoparietal network decreased.

Our results suggest the potential of longitudinal resting state fMRI to delineate regions relevant for disease progression and for diagnostic accuracy, although the direct comparison between our relatively small AD and bvFTD groups did not yield significant group differences in longitudinal changes. Further studies, with larger patient groups, a longer follow-up time, and with more disease progression and neuropsychological decline, may give additional valuable information for disease progression and differential diagnosis.

This is the first study that investigates longitudinal *changes* in functional connectivity in both bvFTD and AD. In bvFTD, we found with the whole-network analysis decreasing longitudinal functional connectivity in the right and left frontoparietal network that encompassed frontal pole, dorsolateral prefrontal cortex, parietal lobule, paracingulate gyrus, and posterior cingulate cortex. In more detail, the network-to-region analysis showed decreased longitudinal connectivity between the left frontoparietal network and the inferior frontal gyrus. Cross-sectional differences in functional connectivity of the inferior frontal gyrus have been found between bvFTD and controls [21].

Furthermore, longitudinal connectivity between the supramarginal gyrus and the right frontoparietal network was decreased over time in bvFTD. The exact role of the supramarginal gyrus in the behavior of bvFTD is not clear. It has been shown that this brain area plays a crucial role in empathy [50], and

gray matter atrophy in the supramarginal gyrus has been reported in bvFTD [51], but is also common in AD [8]. In the present study, we found that in both bvFTD and AD the longitudinal changes in connectivity between the supramarginal gyrus and the right frontoparietal network were significantly different from those in control participants.

In AD, we found decreased longitudinal functional connectivity between the precuneus and the right frontoparietal network. The precuneus is particularly vulnerable for AD pathology, including gray matter atrophy and amyloid pathology [6,52]. Our finding is in line with the observation of decreasing longitudinal connectivity in the precuneus in AD [53].

In addition to the longitudinal changes, we reported cross-sectional group differences at two time points. Although connections with the average time series of the default mode network were not different between AD and controls, we did find group differences in specific regions of this network. Most prominent group differences between AD and controls were higher connectivity between cuneal cortex and the medial visual network, between the paracingulate gyrus and the executive control network, and between the paracingulate gyrus and the salience network. We were able to replicate our baseline findings 1.8 years later at the follow-up measurement. Visual inspection shows more extended group differences at the follow-up measurement, suggesting longitudinal changes in functional connectivity, however, these were not significant. Our baseline findings are in line with the observation of higher functional connectivity in the lingual gyrus, cuneal cortex, and salience network in AD [16,54,55], although not consistently observed [14,16]. While most studies reported lower functional connectivity in patients, there is evidence for higher functional connectivity as well [16,54,55].

In bvFTD, we observed lower functional connectivity compared with controls between the angular gyrus and the right frontoparietal network and between the paracingulate gyrus and the default mode network. These findings were comparable with a study that found differences in these functional connections when comparing patients with bvFTD and controls [21]. In our study, we found these

group differences only at follow-up, not at baseline. Furthermore, we were not able to find differences in the salience network connectivity in the bvFTD group. The inability to find baseline group differences in bvFTD is most likely related to the limited statistical power due to the relatively small number of subjects that was included in the bvFTD group. Another potential explanation is that we included less severely affected bvFTD patients, since we only included patients with scans available at both time points (baseline and follow-up). As a consequence, no data were available for the more severely affected subjects that dropped out of the study prematurely.

The most prominent finding in the direct cross-sectional comparison of AD and bvFTD is the lower functional connectivity between the anterior cingulate cortex and the executive control network in bvFTD compared with AD at the follow-up measurement. The anterior cingulate cortex is identified as a region that is among the first affected brain regions in bvFTD [56]. The deficits in social-emotional functions, which are common in bvFTD, rely on structures including the anterior cingulate cortex and frontoinsula [57,58]. Gray matter atrophy in these structures has shown to be more severe in bvFTD than in AD [59]. Cross-sectional group differences in the anterior cingulate cortex are observed as well in the two other resting state fMRI studies that performed the direct comparison of functional connectivity between patients with bvFTD and AD [16,20].

In addition to the longitudinal changes and group differences in functional connectivity, we found differences in gray matter volume between groups and changes in gray matter volume over time. When we correct the functional connectivity analyses for voxel-based gray matter volume, comparable group differences and longitudinal changes in functional connectivity were found, which might suggests that the functional connectivity differences are independent of gray matter volume.

The disease-specific changes in functional connectivity were not associated with changes in cognitive functioning. Lowest scores on a general measurement of cognitive performance (MMSE) [48] were found in patients with AD. As expected, we found over time a decline in MMSE scores in the AD group. Lowest scores on a general measurement of executive functioning (FAB) [49] were found in

the bvFTD group. Although we expect a decline in FAB scores in the bvFTD group, we found this decline in the AD group. AD patients showed low scores in the memory domain, but also in the executive functioning domain. Although executive functioning could be useful to differentiate AD from bvFTD [60,61], executive functioning, measured with FAB, may not discriminate both types of dementia [62,63]. It has been suggested that testing multiple cognitive domains is required to differentiate both types of dementia rather than focus on one cognitive test [63]. This might contribute to the lack of associations between one single measurements of cognitive functioning and changes in functional connectivity. In the current study, diagnoses were established according to the core clinical criteria for probable AD [2] and for bvFTD [3] and were therefore not based on one single neuropsychological test score.

The diagnosis FTD or AD can only be confirmed by post-mortem brain autopsy after death. A limitation of our study is that postmortem data were not available, therefore the possibility of misdiagnosis of the patients cannot be excluded. Nevertheless, all patients underwent an extensive dementia screening and were evaluated in a multidisciplinary panel including clinicians from different centers specialized in dementia. Only dementia patients that fulfilled the most recent clinical criteria for probable AD [2] and bvFTD [3] were included in the present study. Another limitation of our study is the relatively small number of subjects that was included in the bvFTD group. Further studies, with larger patient groups and more disease progression and neuropsychological decline, may give additional valuable information. A further limitation of the current study includes the possible effects of medication on the functional connections in the AD and bvFTD groups.

This longitudinal study showed data that were collected in two centers. The main strength of multicenter studies is the increased generalizability of the study findings. However, multicenter studies have also its limitations, since the data will be less homogeneous than in single center studies. To increase homogeneity between centers in the current study, we evaluated all patients in a multidisciplinary panel including clinicians from different centers specialized in dementia, we used a standardization approach in order to achieve better comparison across voxels, subjects, and centers

[35], and we added center as covariate in all statistical models, following previous approaches [16,64].

To conclude, we used longitudinal resting state fMRI data of patients with AD and patients with bvFTD and found disease-specific brain regions with longitudinal connectivity changes. Over time, functional connectivity between precuneus and the right frontoparietal network decreased in AD, and the connectivity between the inferior frontal gyrus and left frontoparietal network decreased in bvFTD. This suggests the potential of longitudinal resting state fMRI to delineate regions relevant for disease progression and for diagnostic accuracy, although we did not find group differences in longitudinal changes in the direct comparison of AD and bvFTD patients.

Acknowledgements

This work was supported by funding from the Netherlands Initiative Brain and Cognition (NIHC), a part of the Netherlands Organization for Scientific Research (NWO) (grant numbers 05613010 (A. Hafkemeijer) and 05613014 (C. Möller)). S. Rombouts is supported by the Netherlands Organization for Scientific Research (NWO) (Vici project, grant number 016130677). The funding sources had no involvement in study design, in collection, analysis and interpretation of data, in writing the report, and in the decision to submit the article for publication.

A. Hafkemeijer, C. Möller, E. Dopper, L. Jiskoot, A. van den Berg-Huysmans, J. van Swieten, Y. Pijnenburg, J. van der Grond, and S. Rombouts report no conflicts of interest.

W. van der Flier has received research support from Boehringer Ingelheim, Piramal Imaging, Roche BV, Janssen-Stellar, and speaker honoraria from Boehringer Ingelheim. All funds were paid to her institution.

H. Vrenken has received research support from Merck-Serono, Novartis, and Pfizer, and speaker honoraria from Novartis. All funds were paid to his institution.

F. Barkhof serves / has served on the advisory boards of: Bayer-Schering Pharma, Sanofi-Aventis, Biogen Idec, UCB, Merck-Serono, Novaritis, and Roche. He has been a speaker at symposia organized by the Serono Symposia Foundation. For all his activities he receives no personal compensation.

P. Scheltens serves / has served on the advisory boards of: Genentech, Novaritis, Roche, Danone, Nutricia, Baxter and Lundbeck. He has been a speaker at symposia organized by Lundbeck, Merz, Danone, Novartis, Roche and Genentech. He serves on the editorial board of Alzheimer's Research & Therapy and Alzheimer's Disease and Associated Disorders. And he is a member of the scientific advisory board of the EU Joint Programming Initiative and the French National Plan Alzheimer. For all his activities he receives no personal compensation.

References

[1] Ratnavalli E, Brayne C, Dawson K, Hodges JR (2002) The prevalence of frontotemporal dementia. *Neurology* **58**, 1615–1621.

[2] McKhann GM (2011) Changing concepts of Alzheimer disease. *JAMA* **305**, 2458–2459.

[3] Rascovsky K, Hodges JR, Knopman D, Mendez MF, Kramer JH, Neuhaus J, van Swieten JC, Seelaar H, Dopper EGP, Onyike CU, Hillis AE, Josephs KA, Boeve BF, Kertesz A, Seeley WW, Rankin KP, Johnson JK, Gorno-Tempini M-L, Rosen H, Prioleau-Latham CE, Lee A, Kipps CM, Lillo P, Piguet O, Rohrer JD, Rossor MN, Warren JD, Fox NC, Galasko D, Salmon DP, Black SE, Mesulam M, Weintraub S, Dickerson BC, Diehl-Schmid J, Pasquier F, Deramecourt V, Lebert F, Pijnenburg Y, Chow TW, Manes F, Grafman J, Cappa SF, Freedman M, Grossman M, Miller BL (2011) Sensitivity of revised diagnostic criteria for the behavioural variant of frontotemporal dementia. *Brain* **134**, 2456–2477.

[4] McMillan CT, Avants BB, Cook P, Ungar L, Trojanowski JQ, Grossman M (2014) The power of neuroimaging biomarkers for screening frontotemporal dementia. *Hum Brain Mapp* **35**, 4827–4840.

[5] Raamana PR, Rosen H, Miller B, Weiner MW, Wang L, Beg MF (2014) Three-class differential diagnosis among Alzheimer disease, frontotemporal dementia, and controls. *Front Neurol* **5**, 1–15.

[6] Buckner RL, Snyder AZ, Shannon BJ, LaRossa G, Sachs R, Fotenos AF, Sheline YI, Klunk WE, Mathis CA, Morris JC, Mintun MA (2005) Molecular, structural, and functional characterization of Alzheimer's disease: evidence for a relationship between default activity, amyloid, and memory. *J Neurosci* **25**, 7709–7717.

[7] Krueger CE, Dean DL, Rosen HJ, Halabi C, Weiner M, Miller BL, Kramer JH (2010) Longitudinal rates of lobar atrophy in frontotemporal dementia, semantic dementia, and Alzheimer's disease. *Alzheimer Dis Assoc Disord* **24**, 43–48.

[8] Seeley WW, Crawford RK, Zhou J, Miller BL, Greicius MD (2009) Neurodegenerative diseases target large-scale human brain networks. *Neuron* **62**, 42–52.

[9] Barnes J, Godbolt AK, Frost C, Boyes RG, Jones BF, Scahill RI, Rossor MN, Fox NC (2007) Atrophy rates of the cingulate gyrus and hippocampus in AD and FTLD. *Neurobiol. Aging* **28**, 20–8.

[10] Frings L, Yew B, Flanagan E, Lam BYK, Hüll M, Huppertz H-J, Hodges JR, Hornberger M (2014) Longitudinal grey and white matter changes in frontotemporal dementia and Alzheimer's disease. *PLoS One* **9**, 1–8.

[11] Whitwell JL, Jack CR, Parisi JE, Knopman DS, Boeve BF, Petersen RC, Ferman TJ, Dickson DW, Josephs KA (2007) Rates of cerebral atrophy differ in different degenerative pathologies. *Brain* **130**, 1148–1158.

[12] Pievani M, de Haan W, Wu T, Seeley WW, Frisoni GB (2011) Functional network disruption in the degenerative dementias. *Lancet Neurol* **10**, 829–843.

[13] Balthazar MLF, de Campos BM, Franco AR, Damasceno BP, Cendes F (2014) Whole cortical and default mode network mean functional connectivity as potential biomarkers for mild Alzheimer's disease. *Psychiatry Res* **221**, 37–42.

[14] Greicius MD, Srivastava G, Reiss AL, Menon V (2004) Default-mode network activity distinguishes Alzheimer's disease from healthy aging: evidence from functional MRI. *Proc Natl Acad Sci USA* **101**, 4637–4642.

[15] Hafkemeijer A, van der Grond J, Rombouts SA (2012) Imaging the default mode network in aging and dementia. *Biochim Biophys Acta* **1822**, 431–441.

[16] Zhou J, Greicius MD, Gennatas ED, Growdon ME, Jang JY, Rabinovici GD, Kramer JH, Weiner M, Miller BL, Seeley WW (2010) Divergent network connectivity changes in behavioural variant frontotemporal dementia and Alzheimer's disease. *Brain* **133**, 1352–1367.

[17] Agosta F, Sala S, Valsasina P, Meani A, Canu E, Magnani G, Cappa SF, Scola E, Quatto P, Horsfield MA, Falini A, Comi G, Filippi M (2013) Brain network connectivity assessed using graph theory in frontotemporal dementia. *Neurology* **81**, 134–143.

[18] Borroni B, Alberici A, Cercignani M, Premi E, Serra L, Cerini C, Cosseddu M, Pettenati C, Turla M, Archetti S, Gasparotti R, Caltagirone C, Padovani A, Bozzali M (2012) Granulin mutation drives brain damage and reorganization from preclinical to symptomatic FTLD. *Neurobiol Aging* **33**, 2506–2520.

[19] Farb NAS, Grady CL, Strother S, Tang-Wai DF, Masellis M, Black S, Freedman M, Pollock BG, Campbell KL, Hasher L, Chow TW (2013) Abnormal network connectivity in frontotemporal dementia: evidence for prefrontal isolation. *Cortex* **49**, 1856–1873.

[20] Filippi M, Agosta F, Scola E, Canu E, Magnani G, Marcone A, Valsasina P, Caso F, Copetti M, Comi G, Cappa SF, Falini A (2013) Functional network connectivity in the behavioral variant of frontotemporal dementia. *Cortex* **49**, 2389–2401.

[21] Rytty R, Nikkinen J, Paavola L, Abou Elseoud A, Moilanen V, Visuri A, Tervonen O, Renton AE, Traynor BJ, Kiviniemi V, Remes AM (2013) GroupICA dual regression analysis of resting state networks in a behavioral variant of frontotemporal dementia. *Front Hum Neurosci* **7**, 1–10.

[22] McKhann G, Drachman D, Folstein M, Katzman R, Price D, Stadlan EM (1984) Clinical diagnosis of Alzheimer's disease: Report of the NINCDS ADRDA work group under the auspices of department of health and human services task force on Alzheimer's disease. *Neurology* **34**, 939–944.

[23] Fazekas F, Chawluk JB, Alavi A, Hurtig HI, Zimmerman RA (1987) MR signal abnormalities at 1 .5 T in Alzheimer's dementia and normal aging deficiency. *AJNR Am J Neuroradiol* **149**, 351–356.

[24] Smith SM, Jenkinson M, Woolrich MW, Beckmann CF, Behrens TEJ, Johansen-berg H, Bannister PR, Luca M De, Drobnjak I, Flitney DE, Niazy RK, Saunders J, Vickers J, Zhang Y, Stefano N De, Brady JM, Matthews PM (2004) Advances in functional and structural MR image analysis and implementation as FSL. *Neuroimage* **23**, 208–219.

[25] Ashburner J, Friston KJ (2000) Voxel-based morphometry - the methods. *Neuroimage* **11**, 805– 821.

[26] Zhang Y, Brady M, Smith S (2001) Segmentation of brain MR images through a hidden Markov random field model and the expectation-maximization algorithm. *IEEE Trans Med Imaging* **20**, 45–57.

[27] Jenkinson M, Bannister P, Brady M, Smith S (2002) Improved optimization for the robust and accurate linear registration and motion correction of brain images. *Neuroimage* **17**, 825– 841.

[28] Andersson JLR, Jenkinson M, Smith S (2007) Non-linear optimisation. *FMRIB Tech. Rep. TR07JA1 from www.fmrib.ox.ac.uk/analysis/techrep Last accessed June 26, 2015.*

[29] Good CD, Johnsrude IS, Ashburner J, Henson RN, Friston KJ, Frackowiak RS (2001) A voxel-based morphometric study of ageing in 465 normal adult human brains. *Neuroimage* **14**, 21–36.

[30] Nichols TE, Holmes AP (2001) Nonparametric permutation tests for functional neuroimaging: a primer with examples. *Hum Brain Mapp* **15**, 1–25.

[31] Smith SM, Nichols TE (2009) Threshold-free cluster enhancement: addressing problems of smoothing, threshold dependence and localisation in cluster inference. *Neuroimage* **44**, 83–98.

[32] Smith SM (2002) Fast robust automated brain extraction. *Hum Brain Mapp* **17**, 143–155.

[33] Greve DN, Fischl B (2009) Accurate and robust brain image alignment using boundary-based registration. *Neuroimage* **48**, 63–72.

[34] Andersson JLR, Jenkinson M, Smith S (2007) Non-linear registration aka Spatial normalisation. *FMRIB Tech. Rep. TR07JA2 from www.fmrib.ox.ac.uk/analysis/techrep Last accessed June 26, 2015.*

[35] Yan C, Craddock RC, Zuo X-N, Zang Y-F, Milham MP (2013) Standardizing the intrinsic brain: towards robust measurment of inter-individual variation in 1000 functional connectomes. *Neuroimage* **80**, 246–262.

[36] Beckmann CF, Smith SM (2004) Probabilistic independent component analysis for functional magnetic resonance imaging. *IEEE Trans Med Imaging* **23**, 137–152.

[37] Salimi-Khorshidi G, Douaud G, Beckmann CF, Glasser MF, Griffanti L, Smith SM (2014) Automatic denoising of functional MRI data: combining independent component analysis and hierarchical fusion of classifiers. *Neuroimage* **90**, 449–468.

[38] Filippini N, MacIntosh BJ, Hough MG, Goodwin GM, Frisoni GB, Smith SM, Matthews PM, Beckmann CF, Mackay CE (2009) Distinct patterns of brain activity in young carriers of the APOE-epsilon4 allele. *Proc Natl Acad Sci USA* **106**, 7209–7214.

[39] Hafkemeijer A, Altmann-Schneider I, Oleksik AM, van de Wiel L, Middelkoop HA, van Buchem MA, van der Grond J, Rombouts SA (2013) Increased functional connectivity and brain atrophy in elderly with subjective memory complaints. *Brain Connect* **3**, 353–362.

[40] Khalili-Mahani N, Zoethout RMW, Beckmann CF, Baerends E, de Kam ML, Soeter RP, Dahan A, van Buchem MA, van Gerven JMA, Rombouts SA (2012) Effects of morphine and alcohol on functional brain connectivity during "resting state": a placebo-controlled crossover study in healthy young men. *Hum Brain Mapp* **33**, 1003–1018.

[41] Damoiseaux JS, Rombouts SARB, Barkhof F, Scheltens P, Stam CJ, Smith SM, Beckmann CF (2006) Consistent resting-state networks across healthy subjects. *Proc Natl Acad Sci USA* **103**, 13848–13853.

[42] Beckmann CF, Deluca M, Devlin JT, Smith SM (2005) Investigations into resting-state connectivity using independent component analysis. *Phil Trans R Soc B* **360**, 1001–1013.

[43] Khalili-Mahani N, van Osch MJ, de Rooij M, Beckmann CF, Van Buchem MA, Dahan A, van Gerven JM, Rombouts SA (2014) Spatial heterogeneity of the relation between resting-state connectivity and blood flow: an important consideration for pharmacological studies. *Hum Brain Mapp* **35**, 929–942.

[44] Seeley WW, Menon V, Schatzberg AF, Keller J, Glover GH, Kenna H, Reiss AL, Greicius MD (2007) Dissociable intrinsic connectivity networks for salience processing and executive control. *J Neurosci* **27**, 2349–2356.

[45] Birn RM (2012) The role of physiological noise in resting-state functional connectivity. *Neuroimage* **62**, 864–870.

[46] Fox MD, Snyder AZ, Vincent JL, Corbetta M, Van Essen DC, Raichle ME (2005) The human brain is intrinsically organized into dynamic, anticorrelated functional networks. *Proc Natl Acad Sci USA* **102**, 9673–9678.

[47] Cole DM, Smith SM, Beckmann CF (2010) Advances and pitfalls in the analysis and interpretation of resting-state fMRI data. *Front Syst Neurosci* **4**, 1–15.

[48] Folstein MF, Folstein SE, McHugh PR (1975) Mini-mental state: a practical method for grading the cognitive state of patients for the clinician. *J Psychiat Res* **12**, 189–198.

[49] Dubois B, Slachevsky A, Litvan I, Pillon B (2000) The FAB: A frontal assessment battery at bedside. *Neurology* **55**, 1621–1626.

[50] Silani G, Lamm C, Ruff CC, Singer T (2013) Right supramarginal gyrus is crucial to overcome emotional egocentricity bias in social judgments. *J Neurosci* **33**, 15466–15476.

[51] Lillo P, Mioshi E, Burrell JR, Kiernan MC, Hodges JR, Hornberger M (2012) Grey and white matter changes across the amyotrophic lateral sclerosis-frontotemporal dementia continuum. *PLoS One* **7**, 1–10.

[52] Jack CR, Knopman DS, Jagust WJ, Shaw LM, Aisen PS, Weiner MW, Petersen RC, Trojanowski JQ (2010) Hypothetical model of dynamic biomarkers of the Alzheimer's pathological cascade. *Lancet Neurol* **9**, 119–28.

[53] Damoiseaux JS, Prater KE, Miller BL, Greicius MD (2012) Functional connectivity tracks clinical deterioration in Alzheimer's disease. *Neurobiol Aging* **33**, 19–30.

[54] He Y, Wang L, Zang Y, Tian L, Zhang X, Li K, Jiang T (2007) Regional coherence changes in the early stages of Alzheimer's disease: a combined structural and resting-state functional MRI study. *Neuroimage* **35**, 488–500.

[55] Wang K, Liang M, Wang L, Tian L, Zhang X, Li K, Jiang T (2007) Altered functional connectivity in early Alzheimer's disease: a resting-state fMRI study. *Hum Brain Mapp* **28**, 967–978.

[56] Seeley WW, Crawford R, Rascovsky K, Kramer JH, Weiner M, Miller BL, Gorno-Tempini ML (2008) Frontal paralimbic network atrophy in very mild behavioral variant frontotemporal dementia. *Arch Neurol* **65**, 249–255.

[57] Broe M, Hodges JR, Schofield E, Shepherd CE, Kril JJ, Halliday GM (2003) Staging disease severity in pathologically confirmed cases of frontotemporal dementia. *Neurology* **60**, 1005–1011.

[58] Rosen HJ, Gorno-Tempini ML, Goldman WP, Perry RJ, Schuff N, Weiner M, Feiwell R, Kramer JH, Miller BL (2002) Patterns of brain atrophy in frontotemporal dementia and semantic dementia. *Neurology* **58**, 198–208.

[59] Rabinovici GD, Seeley WW, Kim EJ, Gorno-Tempini ML, Rascovsky K, Pagliaro TA, Allison SC, Halabi C, Kramer JH, Johnson JK, Weiner MW, Forman MS, Trojanowski JQ, DeArmond SJ, Miller BL, Rosen HJ (2008) Distinct MRI atrophy patterns in autopsy-proven Alzheimer's disease and frontotemporal lobar degeneration. *Am J Alzheimers Dis Other Demen* **22**, 474–488.

[60] Iavarone A, Ronga B, Pellegrino L, Loré E, Vitaliano S, Galeone F, Carlomagno S (2004) The Frontal Assessment Battery (FAB): normative data from an Italian sample and performances of patients with Alzheimer's disease and frontotemporal dementia. *Funct Neurol* **19**, 191–195.

[61] Slachevsky A, Villalpando JM, Sarazin M, Hahn-Barma V, Pillon B, Dubois B (2004) Frontal assessment battery and differential diagnosis of frontotemporal dementia and Alzheimer disease. *Arch Neurol* **61**, 1104–1107.

[62] Castiglioni S, Pelati O, Zuffi M, Somalvico F, Marino L, Tentorio T, Franceschi M (2006) The frontal assessment battery does not differentiate frontotemporal dementia from Alzheimer's disease. *Dement Geriatr Cogn Disord* **22**, 125–131.

[63] Lipton AM, Ohman KA, Womack KB, Hynan LS, Ninman ET, Lacritz LH (2005) Subscores of the FAB differentiate frontotemporal lobar degeneration from AD. *Neurology* **65**, 726–731.

[64] Kim D Il, Mathalon DH, Ford JM, Mannell M, Turner JA, Brown GG, Belger A, Gollub R, Lauriello J, Wible C, O'Leary D, Lim K, Toga A, Potkin SG, Birn F, Calhoun VD (2009) Auditory oddball deficits in schizophrenia: an independent component analysis of the fMRI multisite function BIRN study. *Schizophr Bull* **35**, 67–81.

Table 1 Characteristics of the study population

Characteristic	AD (n=20)		bvFTD (n=12)		HC (n=22)	
Age (years)	65.1 (8.0)		64.7 (5.4)		63.8 (5.0)	
Follow-up time (years)	1.79 (0.43)		1.76 (0.43)		1.77 (0.59)	
Gender (male/female)	16/4		9/3		14/8	
Study center (VUMC/LUMC)[a]	16/4		8/4		12/10	
Level of education[b]	4.9 (1.1)		5.0 (1.3)		5.6 (0.7)	
Duration of symptoms (median ± min/max) (months)	36 ± 12/108		60 ± 12/192		n/a	
	Baseline	**Follow-up**	**Baseline**	**Follow-up**	**Baseline**	**Follow-up**
MMSE (max score: 30)	23.2 (2.9)	19.8 (5.2)[I]	24.3 (3.9)	20.9 (6.7)	29.1 (0.9)	29.0 (1.5)
FAB (max score: 18)	14.1 (2.7)	11.7 (3.7)[I]	13.3 (2.7)	10.5 (6.3)	17.4 (1.2)	17.2 (1.1)
CDR (max score: 3)	1.1 (0.8)	1.2 (0.5)	1.3 (0.8)	1.7 (0.8)	0.0 (0.0)	0.0 (0.0)
GDS (max score: 15)	2.7 (3.4)	1.9 (2.0)	1.4 (0.8)	2.7 (3.5)	1.2 (1.2)	0.8 (1.4)

Abbreviations: AD = Alzheimer's disease; bvFTD = behavioral variant of frontotemporal dementia; HC = healthy controls; MMSE = Mini-Mental State Examination; FAB = Frontal Assessment Battery; CDR = Clinical Dementia Rating Scale; GDS = Geriatric Depression Scale

Values are means (standard deviation) for continuous variables or numbers for dichotomous variables. Scores on FAB and GDS were missing in 5 patients.

[a]Imaging was performed either in the Alzheimer Center of the VU University Medical center (VUMC) or in the Leiden University Medical Center (LUMC) in the Netherlands.

[b]Level of education was determined on a Dutch 7-point scale ranging from 1 (less than elementary school) to 7 (university or technical college).

[I] Significant differences between baseline and follow-up

Table 2 Group differences in network-to-region connectivity at baseline and at follow-up

Network and contrast	Brain structure[a]	Side	Peak voxel coordinates (MNI)			Peak T score	
			x	y	z	GM un-corrected	GM corrected
Group differences at baseline							
Medial visual network (I) AD > HC	Lingual gyrus	R	10	-74	0	4.32	5.49
Auditory system network (III) AD > HC	Central opercular cortex	R	56	4	2	4.51	5.16
Executive control network (VI) AD > HC	Paracingulate gyrus	L	-12	44	18	4.23	4.73
Salience network (IX) AD > HC	Paracingulate gyrus	L	-10	20	36	4.26	3.50
Group differences at follow-up							
Medial visual network (I) AD > HC	Lingual gyrus Cuneal cortex	R R	18 18	-70 -80	-4 28	4.82 3.87	5.34 3.87
Auditory system network (III) AD > HC	Planum polare	L	-48	-14	-4	5.24	4.90
Executive control network (VI) AD > HC	Paracingulate gyrus	R	6	50	26	4.08	4.82
Right frontoparietal network (VII) AD < HC	Angular gyrus	R	58	-52	50	4.54	3.63
Salience network (IX) AD > HC	Paracingulate gyrus Anterior cingulate gyrus	R	4	42	30	5.32	6.28
Default mode network (V) bvFTD < HC	Paracingulate gyrus	R	10	52	-4	4.48	3.87
Right frontoparietal network (VII) bvFTD < HC	Angular gyrus	R	56	-52	48	4.47	3.76
Medial visual network (I) bvFTD < AD	Lateral occipital cortex Lateral occipital cortex	R L	24 -18	-72 -82	28 26	4.50 3.72	3.80 3.72
Executive control network (VI) bvFTD < AD	Anterior cingulate gyrus Anterior cingulate gyrus	R L	6 -12	-10 -2	38 38	4.61 3.97	4.41 3.97

Abbreviations: MNI = Montreal Neurological Institute Montreal, QC, Canada; GM = gray matter; AD = Alzheimer's disease; HC = healthy controls; bvFTD = behavioral variant frontotemporal dementia; R = right; L = left

[a]Full list of structures with group differences in network-to-region connectivity (Fig. 4). Between group effects are independent of physiological noise, age, gender, study center, duration of symptoms. Analyses were performed with and without voxel-based gray matter (GM) volume correction (two right columns). Thresholding using $p < 0.05$, FWE corrected, based on the TFCE statistic image. For each peak voxel x-, y-, and z-coordinates in the MNI-152 standard space image are given.

Supplementary Table 1 Neuropsychological performance

Characteristic		AD (n=20)	bvFTD (n=12)	HC (n=22)
MMSE	Baseline	23.2 (2.9) [I]	24.3 (3.9)	29.1 (0.9)
max score 30	Follow-up	19.8 (5.2) [I]	20.9 (6.7)	29.0 (1.5)
FAB	Baseline	14.1 (2.7) [I]	13.3 (2.7)	17.4 (1.2)
max score 18	Follow-up	11.7 (3.7) [I]	10.5 (6.3)	17.2 (1.1)
CDR	Baseline	1.1 (0.8)	1.3 (0.8)	0.0 (0.0)
max score 3	Follow-up	1.2 (0.5)	1.7 (0.8)	0.0 (0.0)
GDS	Baseline	2.7 (3.4)	1.4 (0.8)	1.2 (1.2)
max score 15	Follow-up	1.9 (2.0)	2.7 (3.5)	0.8 (1.4)
RAVLT immediate recall	Baseline	22.8 (8.9)	25.1 (5.7)	45.4 (9.4)
max score 75	Follow-up	18.0 (8.9)	24.8 (14.5)	49.0 (8.9)
RAVLT delayed recall	Baseline	1.8 (1.9)	2.1 (2.3)	8.6 (2.8)
max score 15	Follow-up	1.4 (1.9)	2.5 (3.3)	9.5 (2.9)
VAT	Baseline	2.6 (1.7) [I, II]	4.2 (1.5) [I, II]	5.7 (0.4)
max score 6	Follow-up	1.5 (1.6) [I]	2.2 (1.8) [I]	5.8 (0.4)
Digit span, forward	Baseline	10.1 (3.1)	12.2 (4.6)	12.1 (3.6)
max score 30	Follow-up	9.3 (3.2)	10.8 (5.3)	10.4 (4.0)
Digit span, backward	Baseline	6.2 (2.7)	8.2 (3.4)	8.6 (3.5)
max score 30	Follow-up	5.5 (2.3) [II]	7.1 (4.2) [II]	9.2 (3.3)
TMT A	Baseline	53.5 (21.4)	44.3 (18.9)	37.9 (15.4)
time in seconds	Follow-up	65.8 (32.4)	53.9 (22.6)	36.8 (14.8)
TMT B	Baseline	102.8 (37.9)	93.9 (27.3)	81.1 (29.2)
time in seconds	Follow-up	141.8 (57.7)	112.1 (28.8)	82.7 (31.8)
Stroop I	Baseline	55.4 (12.4)	46.3 (12.5)	46.7 (7.1)
time in seconds	Follow-up	61.1 (16.6)	51.9 (14.5)	47.5 (7.5)
Stroop II	Baseline	77.2 (34.4)	58.1 (9.8)	60.7 (9.7)
time in seconds	Follow-up	90.6 (22.8)	66.1 (7.0)	60.0 (8.7)
Stroop III	Baseline	133.3 (29.8)	102.6 (30.0)	97.3 (19.8)
time in seconds	Follow-up	156.2 (30.7) [II]	110.4 (23.0) [II]	94.9 (20.6)
Categorical fluency	Baseline	14.2 (4.1) [I]	15.5 (5.1)	22.6 (5.4)
responses in 1 minute	Follow-up	9.9 (5.7) [I, II]	16.6 (10.7) [II]	23.2 (6.6)
Letter fluency	Baseline	9.2 (3.4)	8.3 (4.9)	12.6 (4.6)
responses in 1 minute	Follow-up	8.7 (4.2)	9.2 (3.6)	14.3 (3.8)
LDST	Baseline	19.5 (7.0) [II]	27.8 (5.5) [II]	34.1 (6.5)
responses in 1 minute	Follow-up	14.0 (8.6)	22.0 (7.8)	34.7 (6.0)

Abbreviations: AD = Alzheimer's disease; bvFTD = behavioral variant frontotemporal dementia; HC = healthy controls; MMSE = Mini-Mental State Examination; FAB = Frontal Assessment Battery; CDR = Clinical Dementia Rating Scale; GDS = Geriatric Depression Scale; RAVLT = Rey Auditory Verbal Learning Test; VAT = Visual Association Test; TMT = Trail Making Test; LDST = Letter Digit Substitution Test

[I] Significant differences between baseline and follow-up

[II] Significant differences between AD and bvFTD

Figure legends

Figure 1 The four main analyses of this study

This hypothetical model is intended to show the four main analyses performed in the current study. Data points reflect examples of functional connectivity in patients with Alzheimer's disease (AD), patients with behavioral variant frontotemporal dementia (FTD), and healthy controls (HC) at two time points (baseline and follow-up). We have studied 1) cross-sectional group differences at baseline, 2) cross-sectional group differences at follow-up, 3) longitudinal changes within groups (i.e., is functional connectivity at follow-up different from that at baseline (delta)?), 4) group differences in longitudinal changes (i.e., are the deltas different between groups?).

Figure 2 Group differences and longitudinal changes in gray matter volume

Differences in gray matter volume between Alzheimer's disease (AD), behavioral variant frontotemporal dementia (FTD), and healthy controls (HC) (TFCE, FWE-corrected, $p < 0.01$). Images are overlaid on the most informative sagittal, coronal, and axial slices of the MNI-152 standard anatomical image (x, y, and z coordinates of each slice are given). At baseline, A) patients with AD showed less gray matter in precuneal cortex, posterior cingulate cortex, frontal medial cortex, temporal gyrus, hippocampus, and frontal orbital cortex compared with controls and B) patients with bvFTD showed less gray matter in anterior cingulate cortex, insular cortex, and temporal pole compared with controls. These differences in gray matter volume were also found at follow-up (C-D). Longitudinal changes in gray matter volume were found in E) the precuneal cortex, posterior cingulate cortex, temporal gyrus, parahippocampal gyrus, and accumbens in the AD group and in F) the insular cortex, anterior cingulate cortex, and temporal gyrus in the bvFTD group.

Figure 3 Mean network connectivity in resting state networks of interest

A) Spatial maps of eight predefined resting state networks of interest. Images are overlaid on the most informative sagittal, coronal, and axial slices of the MNI-152 standard anatomical image (x, y, and z coordinates of each slice are given). Images are displayed following the radiological convention,

which means that the left side of the image corresponds to the right hemisphere and vice versa. B) Bar graphs show mean (± standard error) functional connectivity within each resting state network for patients with Alzheimer's disease (AD, blue), patients with behavioral variant frontotemporal dementia (FTD, red), and healthy controls (HC, green) both at baseline and follow-up. Asterisks indicate significant group differences or longitudinal changes (post hoc t-tests, Bonferroni corrected).

Figure 4

Group differences in network-to-region connectivity – uncorrected for gray matter volume

Cross-sectional group differences in functional connectivity between resting state networks (indicated in light orange) and localized brain regions (indicated in yellow-to-red and light-to-dark blue, full list of structures in Table 2), uncorrected for voxel-based gray matter volume (see Supplementary Figure 1 for results corrected for voxel-based gray matter volume). A) Post hoc testing showed at baseline higher connectivity in Alzheimer's disease compared with controls (AD > HC, indicated in yellow-to-red). B) The results of post hoc testing showed that the baseline differences were also present at 1.8-year follow-up measurement. At follow-up, functional connectivity was lower in behavioral variant frontotemporal dementia compared with controls (FTD < HC, indicated in light-to-dark blue), and compared with AD patients (FTD < AD, indicated in light-to-dark blue). F-tests did not show at baseline group differences in networks I, V, VI, VII, which is for illustration purposes illustrated by brains without yellow-to-red and light-to-dark blue colored voxels. P values are color coded from 0.05 FWE corrected (red / dark-blue) to < 0.0001 FWE corrected (yellow / light-blue), uncorrected for gray matter volume. Images are overlaid on the sagittal, coronal, and transverse slices of the MNI-152 standard anatomical image (x, y, and z coordinates of each slice are given). Images are displayed following the radiological convention, which means that the left side of the image corresponds to the right hemisphere and vice versa.

Figure 5 Longitudinal changes in network-to-region connectivity within a group

Longitudinal changes in functional connectivity between the right frontoparietal network (indicated in light orange) and A) precuneus in Alzheimer's disease (AD, blue) and B) supramarginal gyrus (FTD,

red) and C) between the left frontoparietal network (indicated in light orange) inferior frontal gyrus in behavioral variant frontotemporal dementia (FTD, red) (uncorrected for gray matter volume). Images are overlaid on the MNI-152 standard anatomical image (coordinates of each slice are given). Images are displayed following the radiological convention, which means that the left side of the image corresponds to the right hemisphere and vice versa. D) Graphs are included to show the directionality of the effects. This shows decreased longitudinal functional connectivity in AD (blue) and FTD (red).

Figure 6 Group differences in longitudinal changes in network-to-region connectivity

Group differences in longitudinal changes in functional connectivity between the right frontoparietal network (indicated in light orange and by roman numerals) and A) the supramarginal gyrus in patients with Alzheimer's disease (AD, blue), and B) the supramarginal gyrus in patients with behavioral variant frontotemporal dementia (FTD, red) compared with healthy controls (HC) (uncorrected for gray matter volume). Images are overlaid on the MNI-152 standard anatomical image (coordinates of each slice are given). Images are displayed following the radiological convention, which means that the left side of the image corresponds to the right hemisphere and vice versa. C) Graphs are included to show the directionality of the effects. This shows group differences in changes in functional connectivity in patients with AD (blue) and in patients with FTD (red) compared with healthy controls (HC, green). The increase in functional connectivity over time in the healthy control group was not significant.

Supplementary Figure 1

Group differences in network-to-region connectivity – corrected for gray matter volume

Cross-sectional group differences in functional connectivity between resting state networks (indicated in light orange) and localized brain regions (indicated in yellow-to-red and light-to-dark blue, full list of structures in Table 2), corrected for voxel-based gray matter (GM) volume. A) Post hoc testing showed at baseline higher connectivity in Alzheimer's disease compared with controls (AD > HC, indicated in yellow-to-red). B) The results of post hoc testing showed that the baseline differences were also present at 1.8-year follow-up measurement. At follow-up, functional connectivity was

lower in behavioral variant frontotemporal dementia compared with controls (FTD < HC, indicated in light-to-dark blue), and compared with AD patients (FTD < AD, indicated in light-to-dark blue). P values are color coded from 0.05 FWE corrected (red / dark-blue) to < 0.0001 FWE corrected (yellow / light-blue), corrected for gray matter volume. Images are overlaid on the sagittal, coronal, and transverse slices of the MNI-152 standard anatomical image (x, y, and z coordinates of each slice are given).

Figure 1 **The four main analyses of this study**

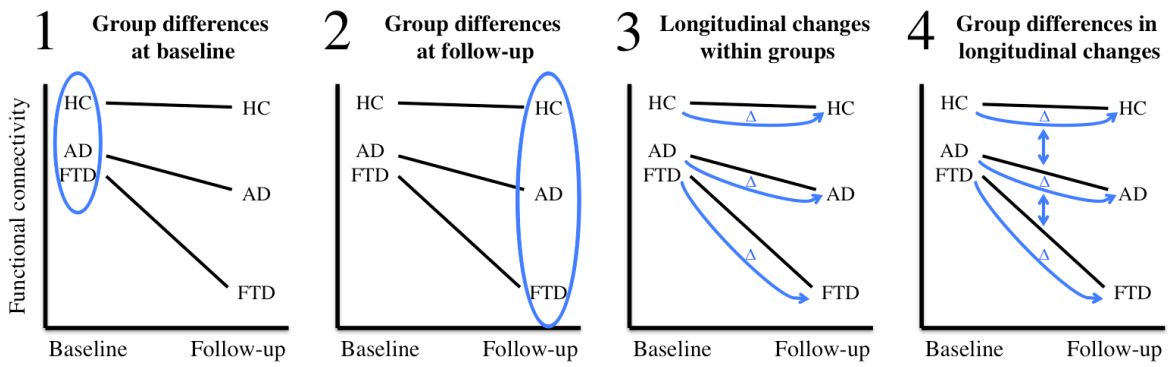

Figure 2 Group differences and longitudinal changes in gray matter volume

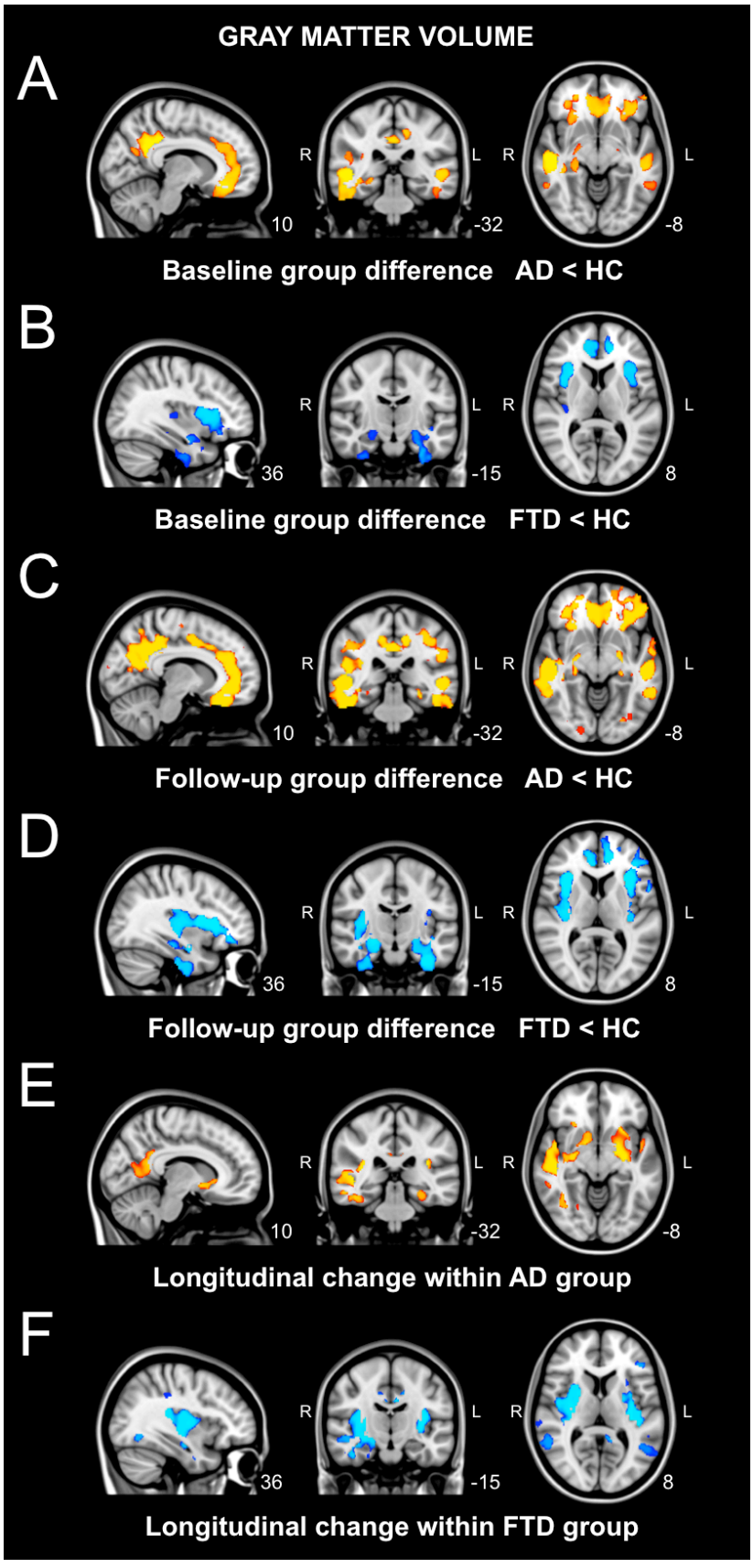

Figure 3 **Mean network connectivity in resting state networks of interest**

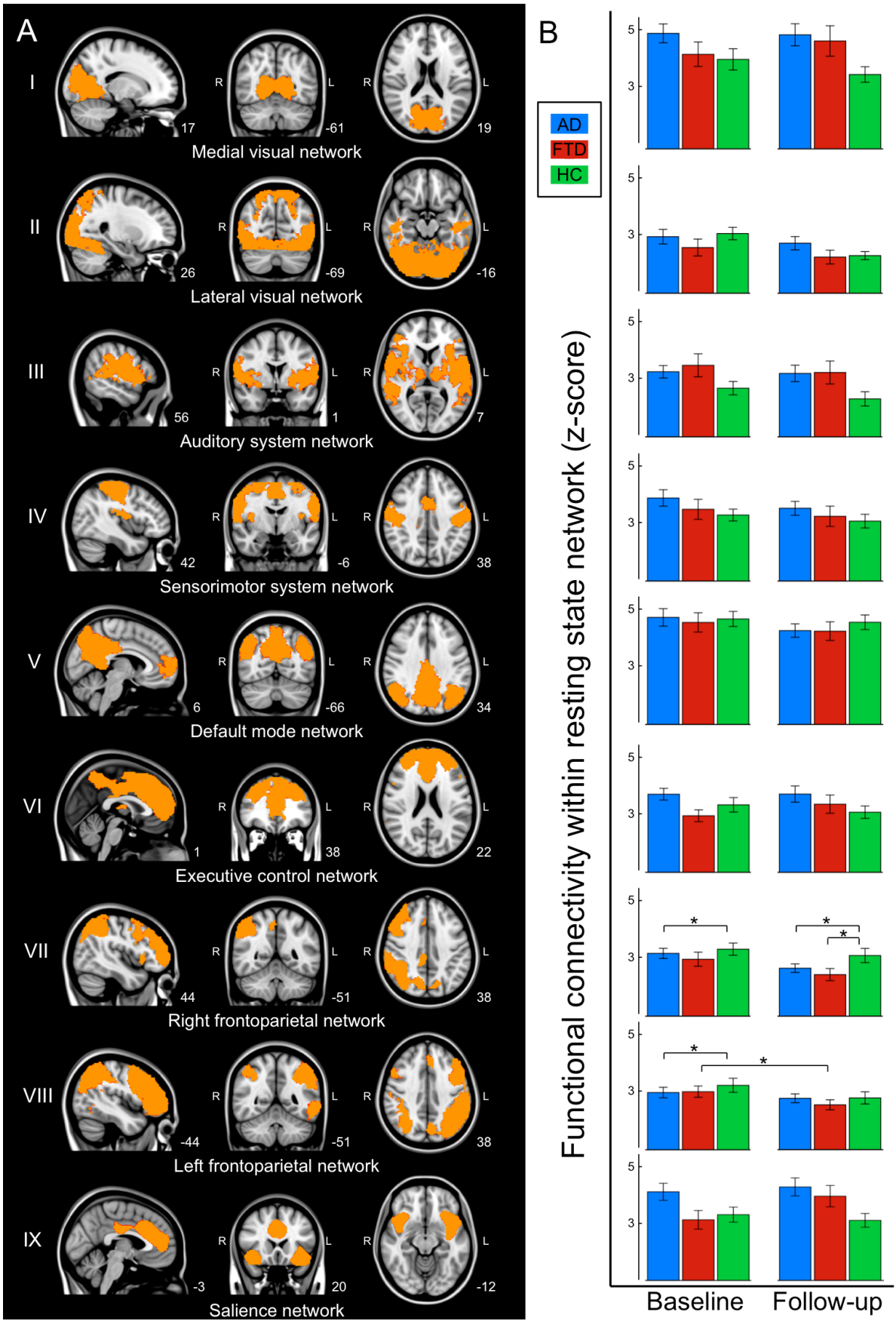

Figure 4

Group differences in network-to-region connectivity - uncorrected for gray matter volume

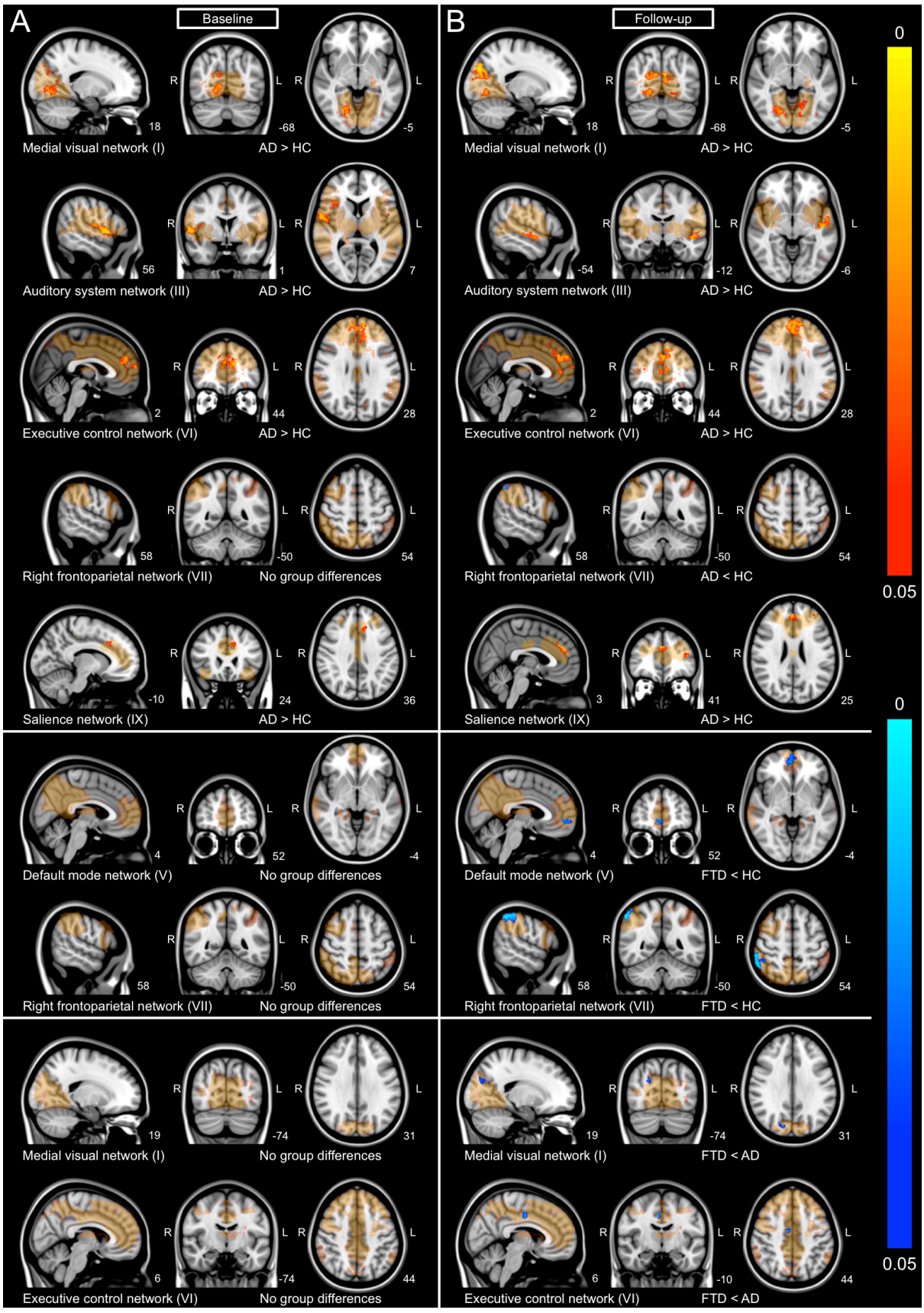

Figure 5 **Longitudinal changes in network-to-region connectivity within a group**

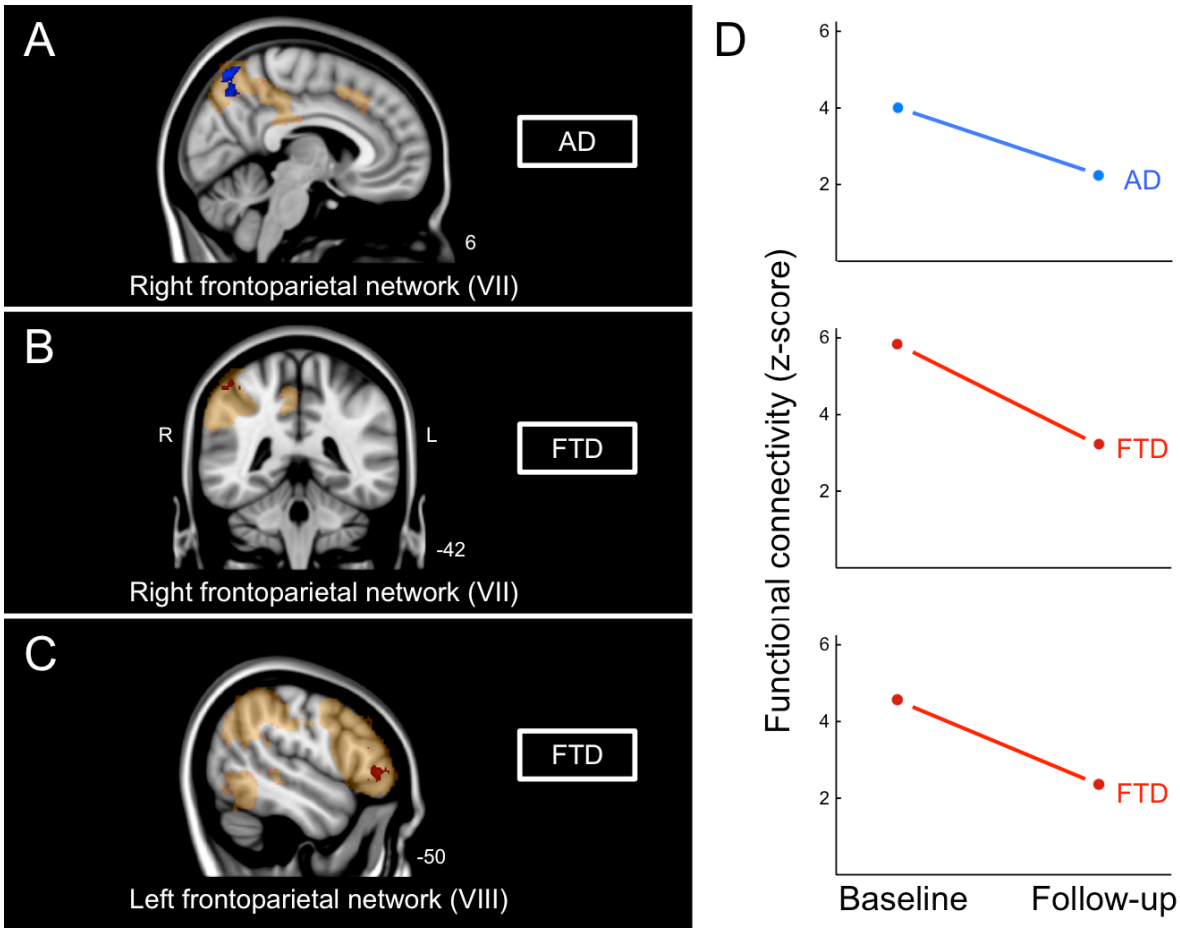

Figure 6 **Group differences in longitudinal changes in network-to-region connectivity**

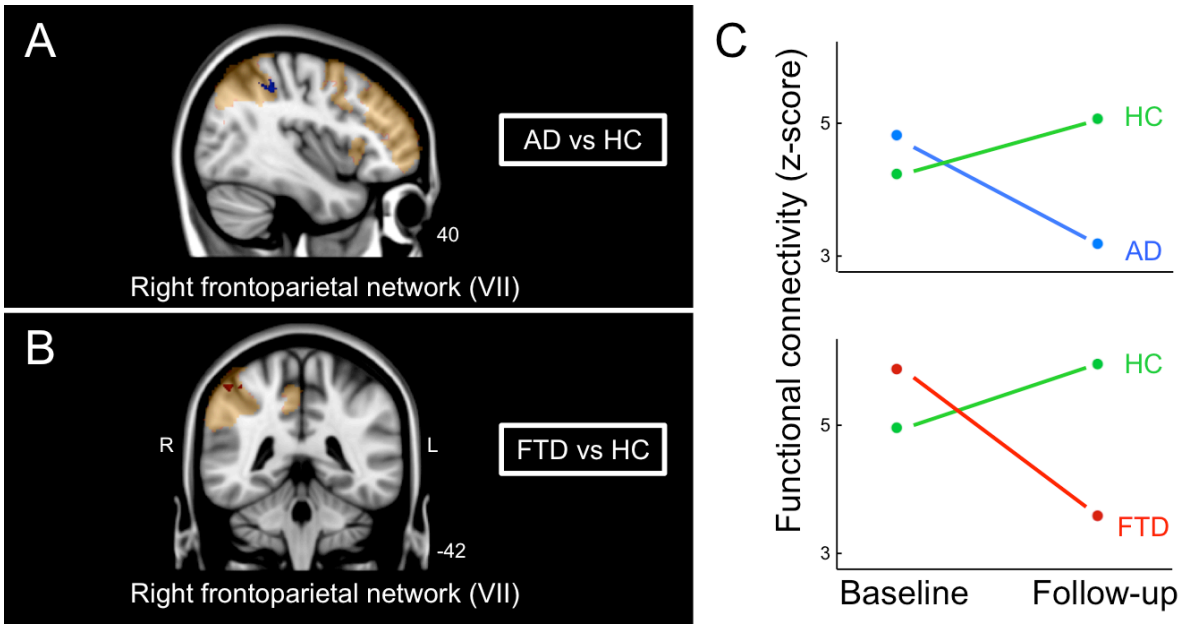

Supplementary Figure 1

Group differences in network-to-region connectivity - corrected for gray matter volume